Journal of Ceramic Processing Research. Vol. 5, No. 4, pp. 337~342 (2004)

J O U R N A L O F
Ceramic Processing Research

Analysis of particle connection in a two-component powder compact by electrical conductivity measurements

Yuki Koreeda, Yoshihiro Hirata* and Soichiro Sameshima

Department of Advanced Nanostructured Materials Science and Technology, Graduate School of Science and Engineering, Kagoshima University, 1-21-40 Korimoto, Kagoshima 890-0065, Japan

Particle connection in a two-component powder compact was quantitatively evaluated by electrical conductivity measurements. As a model system, an alumina powder (median size 0.33 μm, insulator) was mixed with an indium tin oxide powder (ITO, In_2O_3-SnO_2, median size 0.20 μm, electronic conductor) in aqueous solutions at pH 3.0-10.3 to make different types of microstructures of the consolidated powder compacts. The rheological properties of the suspensions and the packing density and electrical conductivity of the powder compacts consolidated by filtration were greatly dominated by the dispersibility of the matrix phase particles (Al_2O_3) rather than by the dispersibility of the second phase particles (ITO). The Al_2O_3-ITO compacts prepared from a well-dispersed suspension at pH 3, showed a high electrical conductivity which was independent of the relative density (60-95%). Particle connection between ITO particles was formed in the consolidated green compacts. The electrical conductivity of the powder compacts processed with a high viscosity suspension at pH 10, was low and enhanced when the bulk density exceeded 60% relative density by sintering. The network of ITO particles was formed by a decrease in the distance between ITO particles during the densification.

Key words: Particle connection, Two-component powder compact, Electrical conductivity, Alumina, Indium tin oxide.

Introduction

The quantitative analysis of the degree of particle mixing in two-component powder compacts is important in order to understand the sintering behavior, mechanical properties or electerical properties of composite materials such as Al_2O_3-ZrO_2 [1], Al_2O_3-TiC [2], Al_2O_3-Ni [3], Si_3N_4-SiC [4] or $3Al_2O_3 \cdot 2SiO_2$-$ZrO_2 \cdot SiO_2$ [5]. In a two-component system of A-B, three types of particle contact of A-A, A-B and B-B are formed in the microstructure of the powder compact [6, 7]. The particle connection provides a geometrical feature of the microdomain. However, it is not easy to evaluate quantitatively the particle connection in the microstructure. In this paper, an evaluation technology using electrical conductivity was studied for the analysis of particle connection of two-component powder compacts. In this study, a model system of Al_2O_3-ITO (Indium Tin Oxide, In_2O_3-SnO_2) was consolidated to understand the microstructure-electrical conductivity relationships. Alumina particles are insulator and ITO particles have a high electronic conductivity. A continuous connection of ITO-ITO particles in the mixed powder compact results in a high electrical conductivity of the powder compact [8, 9]. A homogeneous dispersion of alumina particles around ITO particles interrupts the connection of ITO-ITO particles, resulting in a decreased electrical conductivity. To make different types of microstructures of Al_2O_3-ITO compacts, the two powders were mixed in aqueous suspensions with different pH and consolidated by filtration through gypsum molds. In two-component powder suspensions, (1) the difference of surface characteristics (zeta potential) of each powder, (2) the size ratio between the two kinds of particles and (3) the particle number fraction of the second phase are the main parameters affecting the consolidated microstructures [6, 7, 10]. The consolidated Al_2O_3-ITO compacts were sintered at 1000°-1500 °C in air to understand the influence of bulk density on the microstructure and electrical conductivity.

*Corresponding author:
Tel : +81-99-285-8325
Fax: +81-99-257-4742
E-mail: hirata@apc.kagoshima-u.ac.jp

Experimental Procedure

An ITO powder of 90 mass% In_2O_3-10 mass% SnO_2 system with specific surface area 2.99 m^2/g and primary particle size 0.2 μm, was supplied by Sumitomo Chemical Co., Ltd., Japan. Since particle aggregates were formed in the ITO powder after drying at 100 °C for 24 h, the powder was ground by Y_2O_3 (3 mol%)-stabilized zirconia balls of 3 mm in diameter for 24 h in a polyethylene container. The specific surface area of the milled powder increased to 4.42 m^2/g. An α-Al_2O_3 powder of a specific surface area of 10.5 m^2/g (Al_2O_3 > 99.99 mass%, median size 0.33 μm) was supplied by Sumitomo Chemical Co., Ltd., Japan. The surface characteristics of ITO and Al_2O_3 in dilute aqueous

suspensions were examined by measuring their zeta potentials in 0.01 M-NH_4NO_3 solution (Zeta-Meter Inc., U.S.A.). The pH of each suspension was adjusted using HCl and NH_4OH solutions. The ITO and Al_2O_3 powders were mixed at a volume ratio of ITO/Al_2O_3 = 30/70 in aqueous solutions at pH 3, 6, 8 and 10. The solid content of the suspensions was adjusted to 25 vol%. These suspensions were stirred for 24 h at room temperature and then air bubbles in the suspensions were eliminated for 40 minutes by a vacuum apparatus. The rheological properties of the colloidal suspensions were measured by a viscometer at 20-25 °C (Visconic EHD, Tokimec Inc., Tokyo, Japan). The aqueous suspensions were consolidated by filtration through gypsum molds. The dried compacts were heated at 700 °C for 1 h in air to provide the strength for handling of density measurement, electrical conductivity measurement and microstructural observation. The dried compacts prepared with suspensions at pH 3 and 10 were sintered at 1000°-1500 °C for 1 h in air. The sintered density was measured by the Archimedes method in kerosene. The surfaces of the samples (diameter 10 mm, thickness 1 mm) were polished with No. 2000 SiC abrasive paper and gold was sputtered on the polished surfaces to form thin electrodes. The electrical conductivity of the samples, which were in contact with Pt plates, was measured at 25°-115 °C in air using a two-probe impedance meter in the frequency range from 100 Hz to 1 MHz (Model 4276A, 4277A, Yokogawa Hewlett-Packard Co., Tokyo, Japan) and potentiometer (HA-501G, Hokuto Densi Co., Tokyo, Japan). The microstructures of the samples were observed using a scanning electron microscope (SM-300, Topcon Technologies, Inc., Tokyo, Japan) and electron probe microanalyzer (JXA-8600SX, JEOL, Ltd., Japan).

Experimental Results and Discussion

Surface properties of Al_2O_3 and ITO particles in aqueous suspensions

Fugure 1 shows the zeta potentials of Al_2O_3 and ITO particles as a function of suspension pH. The iso-electric points were pH 8.0 for Al_2O_3 and pH 3.0 for ITO. The suspensions were prepared at pH 3.0 (near the isoelectric point of ITO), pH 6.0 (hetero-coagulation region between Al_2O_3 and ITO), pH 8.0 (near the isoelectric point of Al_2O_3) and pH 10.0 (co-dispersion region of Al_2O_3 and ITO) [11]. Figure 2 shows the possible interactions of Al_2O_3-ITO powder systems at pH 3.0, 6.0, 8.0 and 10.0. The illustration reflects the volume fractions of ITO (30 vol%) and Al_2O_3 (70 vol%) and the particles size ratio (Al_2O_3~0.33 μm, ITO~0.20 μm). At near the isoelectric point of ITO (pH 3.0), ITO particles are flocculated due to van der Waals attractive forces. Electrostatic repulsion acts among the positively charged Al_2O_3 particles. The ITO particles with little charge attract Al_2O_3 particles by van der

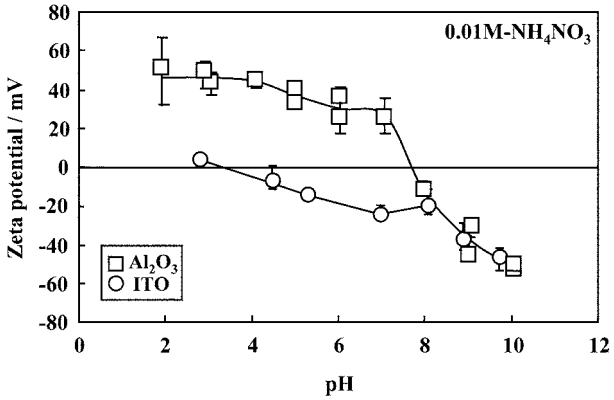

Fig. 1. Zeta potentials of ITO and Al_2O_3 particles as a function of suspension pH.

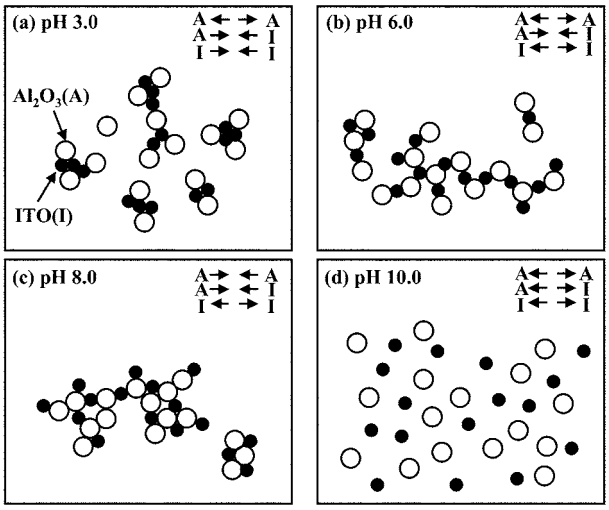

Fig. 2. Schematic illustration of possible interactions of colloidal particles in the Al_2O_3-ITO suspension.

Waals forces. At pH 6.0, the positively charged Al_2O_3 particles are well dispersed by their strong repulsive interaction. The negatively charged ITO particles are adsorbed on the positively charged Al_2O_3 particles by their electrostatic attractive forces. At pH 8.0, near the isoelectric point of alumina, the Al_2O_3 particles become agglomerated due to van der Waals attractive forces. These Al_2O_3 agglomerates are attracted to the negatively charged ITO particles due to the small electrostatic repulsive forces. At pH 10.0, the ITO and Al_2O_3 particles have a similar zeta potential (Fig. 1). These negatively charged particles are co-dispersed due to the strong repulsive energy.

Figure 3 shows the apparent viscosity of the Al_2O_3 (70 vol%)-ITO (30 vol%) suspensions with solid content of 25 vol% at pH 3.3-10.3. The apparent viscosity of the non-Newtonian flow was lower for the acidic suspensions at pH 3.3-6.2 than for the basic suspensions at pH 8.1-10.3. These results were close to the rheological behavior of monolithic alumina suspension, as reported in our previous paper [12]. The rheological properties of the Al_2O_3 (70 vol%)-ITO (30 vol%) suspensions are

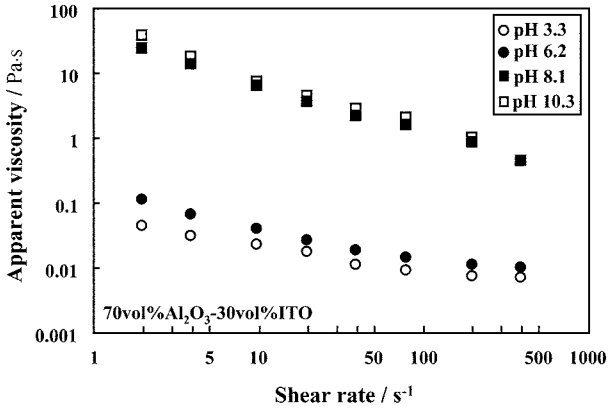

Fig. 3. Apparent viscosity of the Al_2O_3 (70 vol%)-ITO (30 vol%) suspensions with solid content of 25 vol% as a function of shear rate.

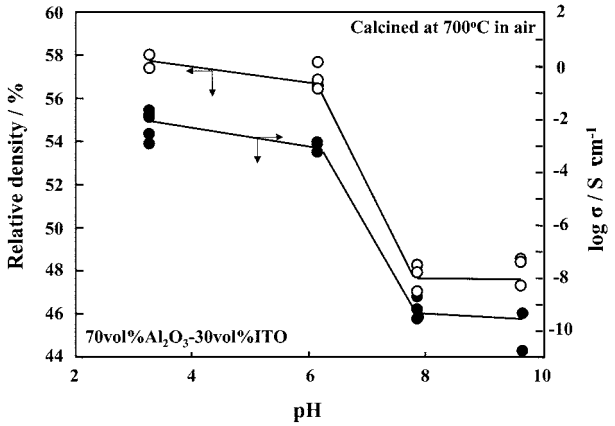

Fig. 4. Relative density and electrical conductivity of the Al_2O_3 (70 vol%)-ITO (30 vol%) compacts as a function of suspension pH.

greatly dominated by the dispersibility of alumina particles. The low apparent viscosity in the acidic suspensions is related to the high dispersibility of alumina particles with high zeta potentials and suggests that the particle connections of ITO-Al_2O_3 and ITO-ITO, as shown in Fig. 2(a), are easily deformed by the applied shear stress. In contrast to the weak agglomeration in the acidic suspensions, the interaction of Al_2O_3-Al_2O_3 became stronger in the basic suspensions as seen in Fig. 3. This phenomenon is explained by the chemical reaction between the hydrated surfaces of Al_2O_3 in the basic solution. The surfaces of alumina particles are covered with hydroxyl units to form $Al(OH)_3$. The agglomeration of Al_2O_3 particles in the basic suspensions proceeds through the chemical reaction between hydrated surfaces, as expressed by Eq. (1) [12],

$$\begin{aligned} &Al(OH)_3 + Al(OH)_3 \rightarrow Al(OH)_2 - O - Al(OH)_2 + H_2O \\ &Al(OH)_2 - O - Al(OH)_2 + Al(OH)_2 - O - Al(OH)_2 \\ &\rightarrow Al(OH)_2 - O - \underset{\displaystyle OH}{\underset{|}{Al}} - O - \underset{\displaystyle OH}{\underset{|}{Al}} - O - Al(OH)_2 + H_2O \end{aligned} \quad (1)$$

Equation (1) is repeated to link three dimensionally. The hydroxyl units remaining in the condensed network provide the negative charge by a chemical reaction with NH_4OH : $Al - OH + NH_4OH \rightarrow Al - O^- + NH_4^+ + H_2O$. As a result, the formation of a particle network through chemical reactions increases the apparent viscosity.

ITO particle connection in the Al_2O_3-ITO compact

Figure 4 shows the relative density of Al_2O_3 (70 vol%)-ITO (30 vol%) compacts consolidated by filtration through gypsum molds as a function of suspension pH. A similar packing property was measured in the monolithic alumina suspensions [12]. The increased density at low pH of the suspensions indicates that the well-dispersed, positively charged alumina particles in the acidic suspensions are densely packed. The decrease of packing density with increasing pH results from the formation of Al_2O_3 agglomeration, as shown in Fig. 3. The formation of particle networks in the basic suspensions reduced the packing density during the filtration of the suspensions.

Figure 4 also shows the electrical conductivity of 70% Al_2O_3-30% ITO compacts as a function of processing pH. The conductivity decreased drastically for the compacts processed with basic suspensions. This result indicates that a continuous particle contact of ITO-ITO was achieved in the compacts processed with the acidic suspensions. As seen in Fig. 4, pH dependence of compact density and conductivity showed a similar tendency. That is, the increased packing density enhances the degree of particle contact of ITO-ITO. The decrease in the packing density expands the distance between ITO and ITO particles. The measured result suggests that the particle network of second phase (ITO) is influenced by the dispersibility of matrix particles (Al_2O_3) rather than the dispersibility of second phase particles.

Figure 5 shows the relative density of 70% Al_2O_3-

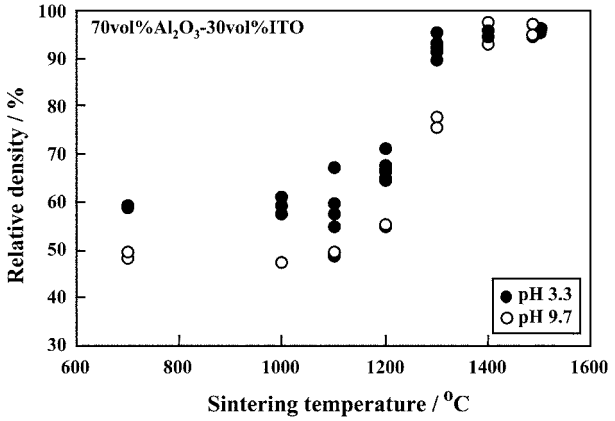

Fig. 5. Relative density of the Al_2O_3 (70 vol%)-ITO (30 vol%) compacts as a function of sintering temperature.

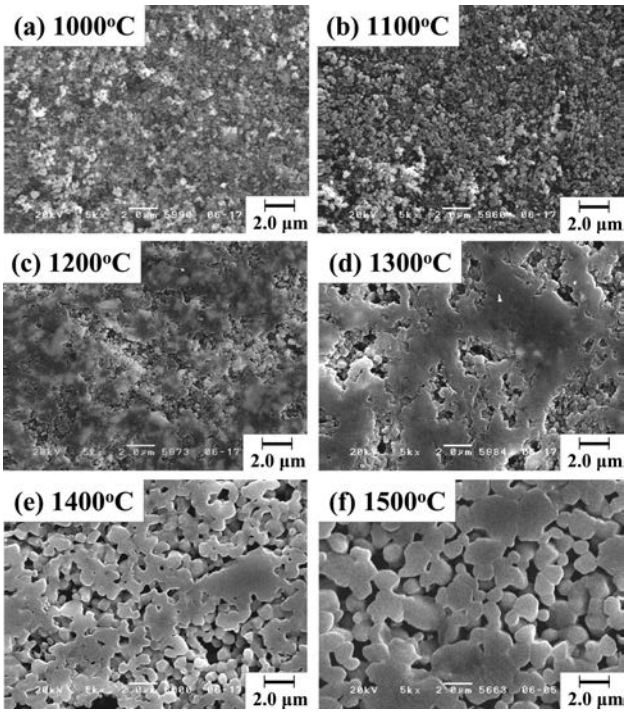

Fig. 6. Microstructures of the Al_2O_3 (70 vol%)-ITO (30 vol%) compacts consolidated from the suspension at pH 3.3 and sintered at (a) 1000 °C, (b) 1100 °C, (c) 1200 °C, (d) 1300 °C, (e) 1400 °C and (f) 1500 °C in air.

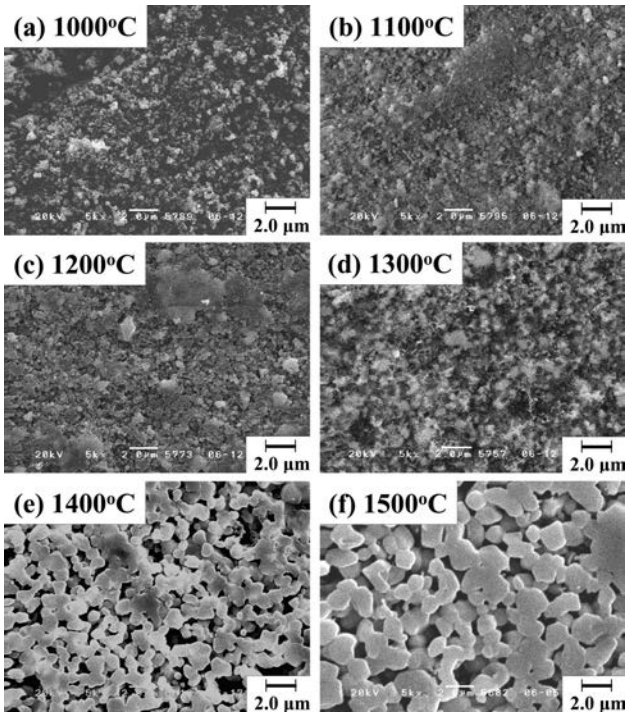

Fig. 7. Microstructures of the Al_2O_3 (70 vol%)-ITO (30 vol%) compacts consolidated from the suspension at pH 9.7 and sintered at (a) 1000 °C, (b) 1100 °C, (c) 1200 °C, (d) 1300 °C, (e) 1400 °C and (f) 1500 °C in air.

30% ITO compacts formed with the aqueous suspensions at pH 3.3 and 9.7, as a function of sintering temperature. Both the bulk densities increased at temperatures above 1200 °C [13, 14]. The sinterability of Al_2O_3-ITO compacts was higher for the compact processed at pH 3.3 than for that processed at pH 9.7. Therefore the dispersibility of colloidal particles affects both the green and sintered densities.

Figures 6 and 7 show the sintered microstructures of the 70% Al_2O_3-30% ITO compacts, processed with the suspensions at pH 3.3 and 9.7, respectively. The densification of ITO and Al_2O_3 particles proceeded with grain growth in the temperature range from 1200° to 1500 °C. The pore size was also enlarged by the grain growth. However, it is difficult to distinguish ITO particles from Al_2O_3 particles in these microstructures. X-ray diffraction patterns of the sintered compacts indicated no formation of the compound of the Al_2O_3-ITO system [15].

Figure 8 shows the electrical conductivity of 70% Al_2O_3-30% ITO compact as a function of sintering temperature. The Al_2O_3-ITO compact prepared with the suspension at pH 3.3, showed a high electrical conductivity, which was almost independent of the relative density (60-95%). On the other hand, the low electrical conductivity of the powder compact processed at pH 9.7 was enhanced when the bulk density exceeded 60% relative density. This result indicates that the densification of particles shortens the distance between ITO

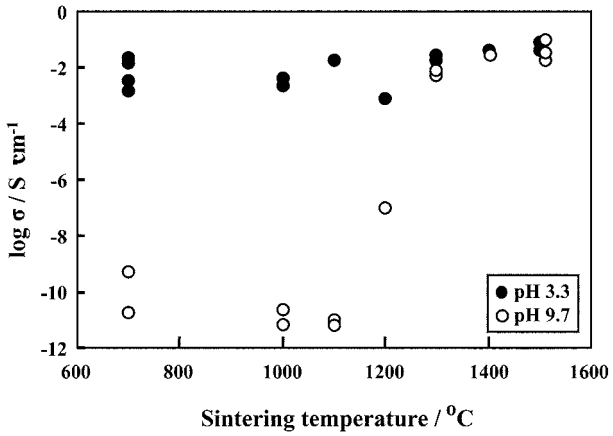

Fig. 8. Electrical conductivity of the Al_2O_3 (70 vol%)-ITO (30 vol%) compacts as a function of sintering temperature.

particles and leads to a continuous particle connection of ITO-ITO. The above results in Figs. 4, 5 and 8 indicate that (1) the high dispersibility of matrix particles (Al_2O_3) in an aqueous suspension enhances the packing density of the Al_2O_3-ITO powders, (2) the increased packing density effectively leads to a connection between second-phase particles (ITO) (3) densification of a low packing density compact by sintering gradually shortens the distance between the second-phase particles, and (4) grain growth during the sintering provides no significant influence on the particle connection of the second phase.

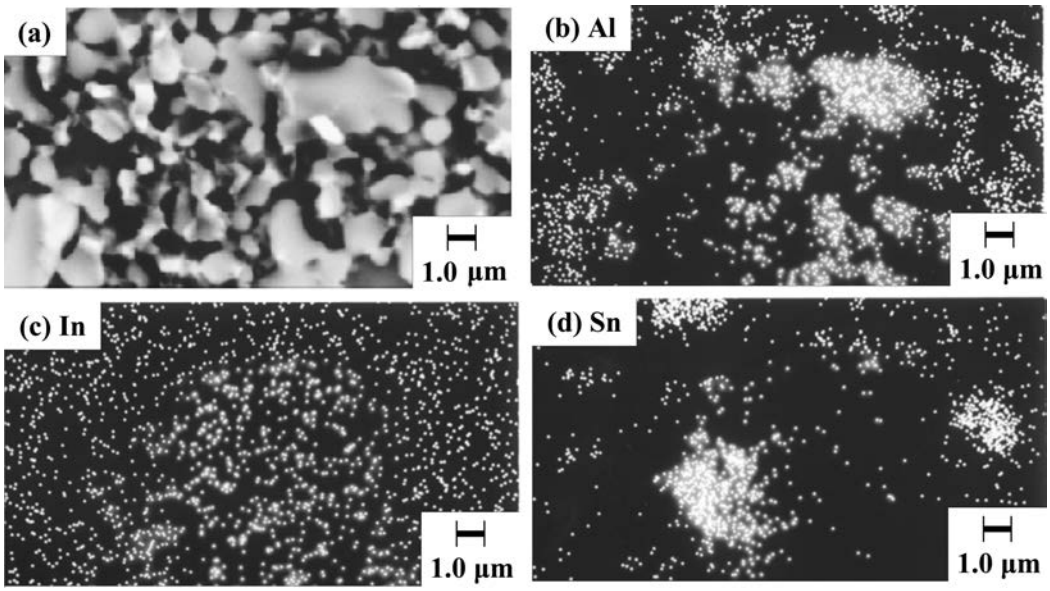

Fig. 9. Microstructure (a) and elemental distribution maps of (b) Al, (c) In and (d) Sn for the Al_2O_3 (70 vol%)-ITO (30 vol%) compacts consolidated from the suspension at pH 3.3 and sintered at 1500 °C in air.

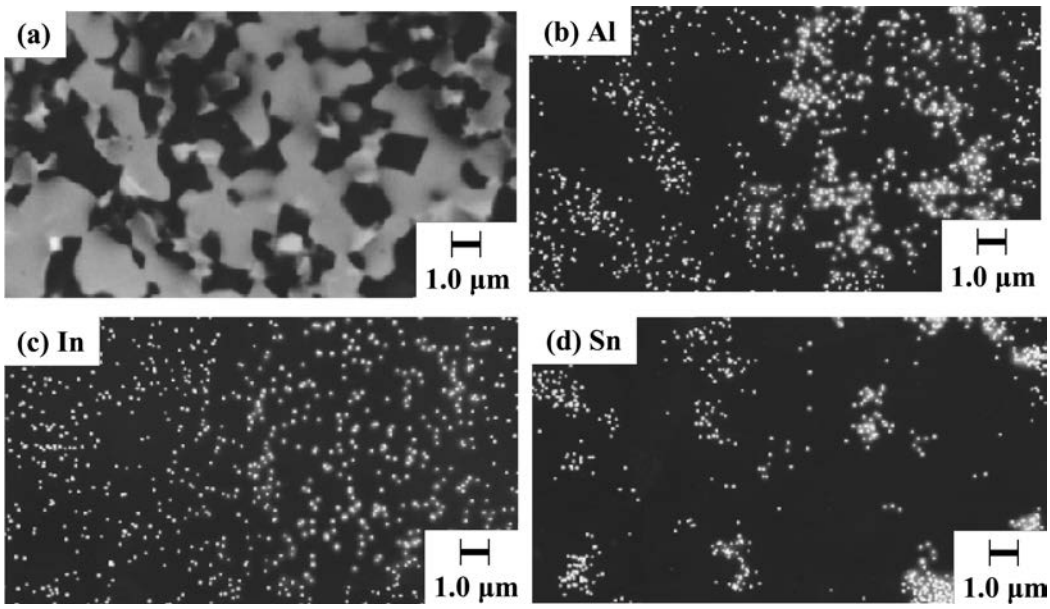

Fig. 10. Microstructure (a) and elemental distribution maps of (b) Al, (c) In and (d) Sn for the Al_2O_3 (70 vol%)-ITO (30 vol%) compacts consolidated from the suspension at pH 9.7 and sintered at 1500 °C in air.

Figures 9 and 10 show (a) microstructures and the elemental distribution maps of (b) Al, (c) In and (d) Sn by electron probe microanalyzer for the 70% Al_2O_3-30% ITO compacts processed with the suspensions at pH 3.3 and pH 9.7, respectively, and sintered at 1500 °C in air. The concentrations of the elements are expressed in terms of brightness in (b), (c) and (d). The Al element was mainly measured on the gray grains and the In element was distributed over the black regions in the microstructure (a). These results indicate that the gray regions correspond to Al_2O_3 grains and the black regions correspond to ITO grains and pores. The ratio of surface area of gray regions (Al_2O_3) to black regions (ITO and pores) (64.2:35.8 for Fig. 9(a), 60.3:39.7 for Fig. 10(a)) and the ratio of surface area of grains (Al_2O_3 and ITO) to pores in Fig. 6(f) (87.2:12.8) and Fig. 7(f) (84.8:15.2) were coupled to determine the Al_2O_3 content in Figs. 9(a) and 10(a): 73.6% Al_2O_3-26.4% ITO for Fig. 9(a), 71.2% Al_2O_3-28.8% ITO for Fig. 10(a). These compositions were close to the mixing volume ratio of the starting Al_2O_3 (70%) and ITO (30%) powders. Therefore, the ITO grains were continuously connected in the black regions in Figs. 9 (a) and 10(a).

Conclusions

(1) An alumina powder with an isoelectric point at pH 8.0 was mixed with an ITO powder with an isoelectric point at pH 3.0 at 30 vol% ITO fraction. The rheological properties of the suspensions were greatly dominated by the dispersibility of alumina particles, depending on the suspension pH.

(2) The Al_2O_3 (70%)-ITO (30%) suspensions were consolidated by filtration through gypsum molds. The particle network of second phase (ITO) in the green compacts, which was evaluated by the packing density and electrical conductivity, was influenced by the dispersibility of matrix particles (Al_2O_3) rather than the dispersibility of the second-phase particles.

(3) The densification of the Al_2O_3-ITO compact proceeded at temperatures above 1200 °C. The Al_2O_3-ITO compact prepared with the well-dispersed suspension at pH 3.3, showed a high electrical conductivity which was independent of the relative density (60-95%), indicating the particle connection of ITO.

(4) The low electrical conductivity of the powder compact processed with a high viscosity suspension at pH 9.7, was enhanced when the bulk density exceeded 60% relative density. The particle network of ITO was gradually formed with a decrease in the distance between ITO particles by sintering.

References

1. C. Kaya, E.G. Butler, and M.H. Lewis, J. Eur. Ceram. Soc. 23 (2003) 935-942.
2. K.F. Cai, D.S. Mclachlan, and R. Manyatsa, Ceram. Inter. 28 (2002) 217-222.
3. G. Li, X. Huang, and J. Guo, Mater. Sci. Eng. A, in press (2003).
4. D. Cheong, K. Hwang, and C. Kim, Composites A 30 (1999) 425-427.
5. G.Y. Lin and T.C. Lei, Ceram. Inter. 24 (1998) 313-326.
6. Y. Hirata and W.H. Shih, Proceedings of 9th CIMTEC-World Ceramics Congress & Forum on New Materials, Part B, Edited by P. Vincenzini, Techna, Faenza (1999) 637-644.
7. Y. Hirata, N. Numaguchi, and W.H. Shih, Key Eng. Mater. 159-160 (1999) 127-134.
8. Ph. Parent, H. Dexpert, G. Tourillon, and J.M. Grimal, J. Electrochem. Soc. 139 (1992) 276-281.
9. Y. Hirata, R. Dong, A. Yoshitomi, K. Hayata, M. Higashi, and K. Saegusa, J. Ceram. Soc. Japan 109 (2001) 49-54.
10. C. Ballario, A. Bonincontro, and C. Cametti, J. Colloid Interface Sci. 72 (1979) 304-313.
11. Y. Hirata, K. Hidaka, H. Matsumura, Y. Fukushige, and S. Sameshima, J. Mater. Res. 12 (1997) 3146-3157.
12. Y. Hirata, X.H. Wang, Y. Hatate, and K. Ijichi, J. Ceram. Soc. Japan 111 (2003) 232-237.
13. B.C. Kim, J.H. Lee, J.J. Kim, and T. Ikegami, Mater. Lett. 52 (2002) 114-119.
14. J.G. Nam, H. Choi, S.H. Kim, K.H. Song, and S.C. Park, Scripta Mater. 44 (2001) 2047-2050.
15. Y. Ohya, T. Ito, M. Kaneko, T. Ban, and Y. Takahashi, J. Ceram. Soc. Japan 108 (2000) 803-806.